

Xianfeng Fan<sup>1</sup> and Ming J. Zuo<sup>2</sup>

# Gearbox Fault Feature Extraction Using Hilbert Transform, S-Transform, and a Statistical Indicator

**ABSTRACT:** Vibration analysis has been widely used in machine fault feature extraction and diagnosis of rotating machinery. The effects of modulation and nonstationarity in vibration signals collected from a faulty gearbox present challenges for fault feature extraction. Hilbert transform and S-transform have the ability to address these issues through demodulation and time-frequency analysis, respectively. In this paper, we propose to use a feature indicator to represent the S-transform coefficients. The proposed method integrates the advantages of Hilbert transform, S-transform, and the proposed feature indicator (FI). The validity of the proposed method is verified with a simulated signal and real gearbox vibration signals. Comparison studies show that the proposed method is more effective and does not require the operators to have a lot of diagnostic experience.

**KEYWORDS:** gearbox, fault features extraction, Hilbert transform, S-transform, feature indicator

## Introduction

Gearboxes are widely used in industrial machinery. These machines are expected to work reliably to prevent accidents and reduce operating costs [1]. Vibration-based signal processing methods have been used in condition monitoring of gearboxes. Effective fault feature extraction methods are needed to identify early fault symptoms and prevent catastrophic failures. The modulation existing in gearbox vibration signals [2–4] and the non-stationarity of the gearbox vibration signals [5–8] should be addressed for effective fault feature extraction in gearbox condition monitoring.

Modulation occurs in gearbox vibration spectra, wherein the gear meshing frequency (the carrier signal) is modulated by the rotating frequency of the gear (the modulating signal). The carrier signal exists whether the gearbox has a fault or not; while the modulating signal is usually a reflection of gear faults. Therefore, identification of the modulating signal helps fault detection. Though the Hilbert transform [2] has been used to extract the modulating signal that reflects the instantaneous characteristics of the impulses generated by a gear fault, it is unable to extract fault features if the modulating signal is very weak. When a gear fault is in its early stage of development, it generates a weak modulating signal. Therefore, the Hilbert transform alone is not always effective for detection of such early faults. In addition, gearbox load, electrical current, and actual faults often make the modulating signal nonstationary [8].

Conventional FFT-based methods are not suitable for analysis of nonstationary signals. Time-frequency analysis methods such as short-time Fourier transform (STFT) [9], Wigner-Ville distribution (WVD) [10], Choi-Williams distribution (CWD) [11], Wavelet

analysis [12,13], and empirical mode decomposition (EMD) [14] have been used for detection of gear faults. However, these methods still have limitations [8,15,16]. The resolution of STFT is constant because the window width is constant. WVD may lead to emergence of negative energy levels that are difficult to explain. CWD is insensitive to the time localization of events. The resolution of wavelet analysis depends on the mother wavelet used. We are unable to specify the frequency bandwidth of each intrinsic mode functions directly using EMD-based methods.

S-transform provides a time-frequency representation with frequency dependent resolutions while, at the same time, maintaining a direct relationship with the Fourier spectrum [17]. The S-transform of a function  $x(t)$  (discrete or continuous) is defined as a continuous wavelet transform (CWT) using a specific mother wavelet multiplied by a phase factor. It has been used in power quality analysis [18]. Based on S-transform, a method called Hilbert and TT-transform (HTT) is proposed to address modulation and nonstationarity issues for fault features extraction [19]. The principle of the proposed method is to analyze the modulating signal created by a gear fault using a time-time representation.

In this paper, we propose a novel feature extraction method for gearbox signal analysis. Hilbert transform is used to extract the modulating signal. S-transform is used to analyze the extracted modulating signal. A feature indicator (FI) based on the three- $\sigma$  concept is used to analyze the S-transform coefficients. The remainder of this paper is organized as follows. Hilbert transform, CWT, and S-transform are briefly introduced in Section II. The feature indicator and the proposed method are outlined in Section III. Simulated and real gearbox vibration signals are analyzed to validate the proposed method in Section IV. Conclusions and discussions are given in Section V.

## Hilbert Transform, Wavelet Transform, and S-Transform

Hilbert transform was first developed to process nonstationary narrow-band signals [20]. It is a time-series analysis technique used

Manuscript received August 11, 2006; accepted for publication February 6, 2007; published online April 2007.

<sup>1</sup>State Key Laboratory of Mechanical System and Vibration, Shanghai Jiao-tong University, Shanghai 200030, P. R. China, e-mail: fanxf@yahoo.com and School of Mechatronics Engineering, University of Electronic Science and Technology of China, Chengdu, Sichuan, 610054, P. R. China.

<sup>2</sup>Department of Mechanical Engineering, University of Alberta, Edmonton, Alberta, T6G 2G8, Canada, e-mail: ming.zuo@ualberta.ca

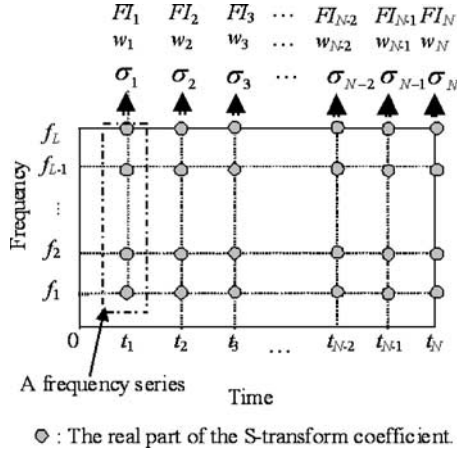


FIG. 1—The calculation of FIs based on S-transform.

to derive amplitude and phase information of a signal as a function of time. For a continuous signal,  $x(t)$ , its Hilbert transform,  $y(t)$ , is defined as

$$y(t) = H[x(t)] = \frac{1}{\pi} \int_{-\infty}^{\infty} \frac{x(t')}{t-t'} dt' \quad (1)$$

Both  $x(t)$  and  $y(t)$  form the so-called analytic signal denoted by  $H(t)$  given by

$$H(t) = x(t) + iy(t) = A(t)e^{i\theta(t)} \quad (2)$$

where  $A(t) = \sqrt{x^2(t) + y^2(t)}$ ,  $\theta(t) = \tan^{-1}y(t)/x(t)$ , and  $i = \sqrt{-1}$ . Using Eq 2, we get the instantaneous envelope (the modulating signal)  $A(t)$  and the phase function  $\theta(t)$ .  $x(t)$  can be analyzed in discrete form for computer programming.

If  $\psi(t)$  is a square integrable complex function and its Fourier transform  $\hat{\psi}(\omega)$  satisfies the admissibility condition

$$C_{\psi} = \int_{-\infty}^{\infty} \frac{|\hat{\psi}(\omega)|^2}{|\omega|} d\omega < \infty \quad (3)$$

we call  $\psi(t)$  the mother wavelet. The corresponding family of wavelets consists of the son wavelets generated through dilation and translation from  $\psi(t)$ , as shown in Eq 4:

$$\psi_{a,\tau}(t) = |a|^{-1/2} \psi\left(\frac{t-\tau}{a}\right) \quad (4)$$

where  $a$  is the scale parameter,  $\tau$  is the time location, and the term  $|a|^{-1/2}$  is used to ensure energy preservation. The CWT of signal  $x(t)$  is defined as [21]:

$$W(a, \tau) = |a|^{-1/2} \int x(t) \psi^*\left(\frac{t-\tau}{a}\right) dt \quad (5)$$

where  $*$  stands for complex conjugate and  $a$  and  $\tau$  may vary continuously. Clearly, the wavelet coefficients,  $W(a, \tau)$ , depend on the mother wavelet used.

The S-transform is defined as a CWT with a specific mother wavelet multiplied by a phase factor. Using  $e^{-i2\pi ft}$  as the phase factor and

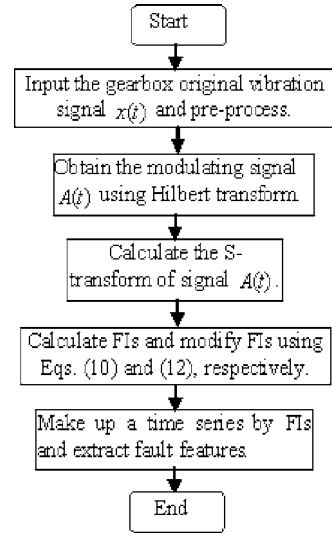


FIG. 2—The procedure of the proposed method.

$$\psi(f) = \frac{|f|}{\sqrt{2\pi}} e^{-(f)^2/2} e^{-i2\pi ft} \quad (6)$$

as the wavelet function, the S-transform of the signal  $x(t)$  can be expressed by [17]

$$S(f, \tau) = \int_{-\infty}^{\infty} x(t) \frac{|f|}{\sqrt{2\pi}} e^{-(\tau-t)^2 f^2/2} e^{-i2\pi ft} dt \quad (7)$$

The S-transform of  $x(t)$  provides a time-frequency representation with frequency-dependent resolution while, at the same time, maintaining a direct relationship with the Fourier spectrum. In the used wavelet function, the dilation factor  $a$  is selected to be the reciprocal of frequency. In Eq 7, the S-transform has a window whose height and width vary with frequency  $f$ . The S-transform is similar to the wavelet transform, except that we substitute  $1/\sqrt{a}$  in CWT by a scaling factor  $|f|$ .

## The Proposed Feature Extraction Method

For time epochs  $t = \{t_1, t_2, \dots, t_N\}$ , we have the original vibration data as  $x(t) = \{x(t_1), x(t_2), \dots, x(t_N)\}$ .  $N$  is the length of the data series. In order to eliminate the trend pattern in the collected data, the original samples are preprocessed by

$$x'(t_j) = x(t_j) - \frac{1}{N} \sum_j x(t_j) \quad (8)$$

where  $x'(t_j)$  is the preprocessed data,  $j = 1, 2, \dots, N$ .

Since the Hilbert transform can extract the envelope (modulating) signal and the S-transform can provide a good representation of the time-frequency properties of a signal, we propose to demodulate the vibration signal  $x'(t)$  using Hilbert transform and obtain the envelope of signal  $x'(t)$ . The obtained envelope signal is then processed with the S-transform. The coefficients of the S-transform are complex. We will use only the real parts of these coefficients. The corresponding matrix of the real parts of these coefficients is given by

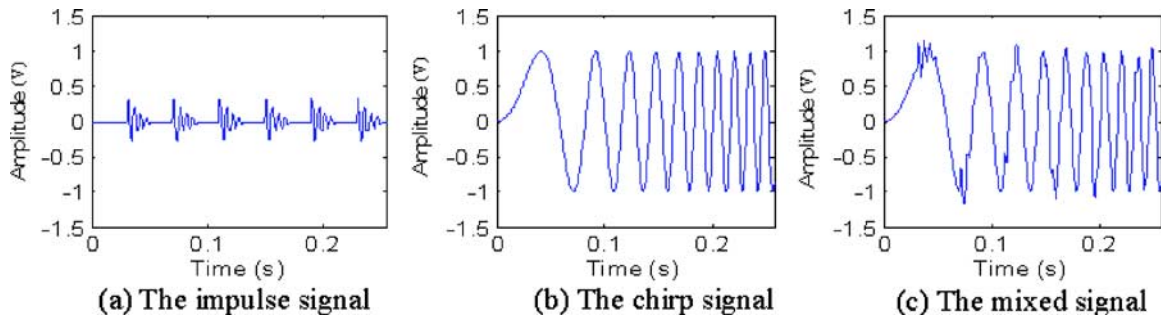


FIG. 3—The simulated signals.

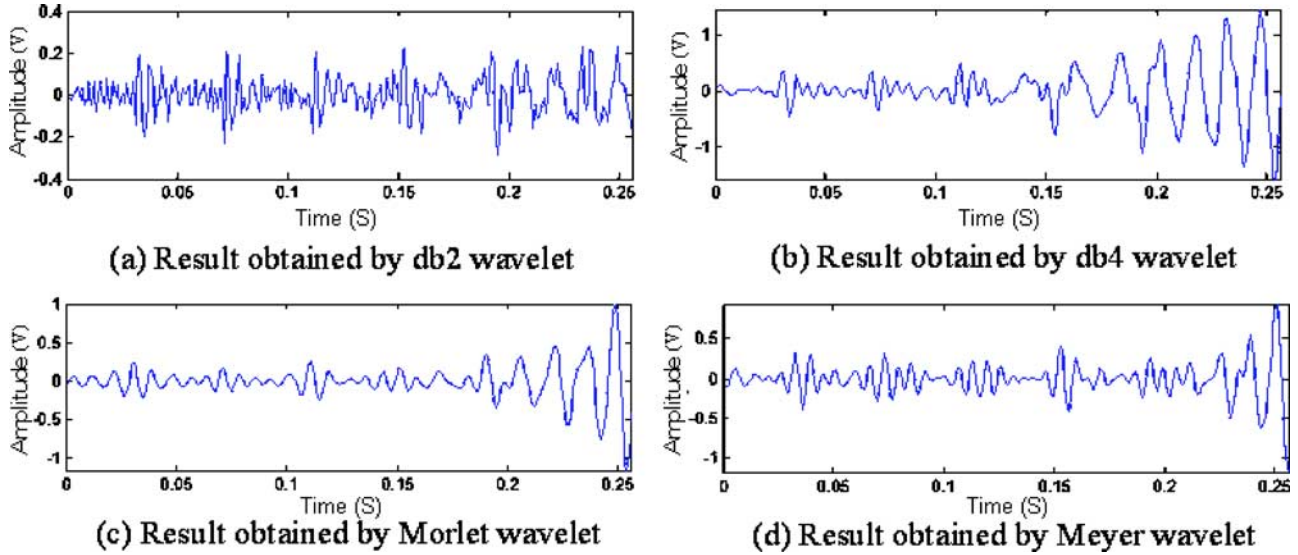


FIG. 4—The analysis results of the simulated signal obtained by the adaptive CWT.

$$S = \{ \text{Re}(S(f_i, t_j)) \mid i = 1, 2, \dots, L; j = 1, 2, \dots, N \} \quad (9)$$

where  $L$  is the length of the frequency components at each time position and  $N$  is the length of the original signal  $x(t)$ . The matrix  $S$  is represented by the circles in Fig. 1. The time scale ranges from 0 to  $t_N$  and  $t_N$  is the duration of signal  $x(t)$ . The frequency scale ranges from 0 to  $f_L$  and  $f_L$  is the highest frequency component determined by sampling frequency.

For a healthy fixed-shaft gearbox, modulation may be caused by other random effects such as minor manufacturing imperfection. The modulating signal is expected to be very weak, remains in a narrow range, and very often follows the Gaussian distribution based on the central limit theorem. Correspondingly, the S-transform coefficients of the modulating signal at each time position is expected to fluctuate within a narrow range following the Gaussian distribution; 99.73 % of these coefficient values are expected to be within three standard deviations of their average value [22]. When a fault is present in the gearbox, we expect to see more of these coefficients to be outside of the three standard deviations of the average value. Based on these arguments, we propose a feature indicator denoted by FI and defined by

$$FI_j = \frac{1}{L} \sum_{i=1}^L I(|a_{ij}| > (\bar{a}_j + 3\sigma_0)) \quad (10)$$

where  $a_{ij} = \text{Re}(S(f_i, t_j))$  at a specific time position  $t_j$ ,  $\bar{a}_j = 1/L \sum_{i=1}^L \text{Re}(S(f_i, t_j))$  at a specific time position  $t_j$ ,  $\sigma_0$  is the baseline standard deviation,  $i$  represents the  $i$ th frequency scale,  $f_i$  represents the  $i$ th frequency component, and  $I(\cdot)$  is a binary indicator function defined as

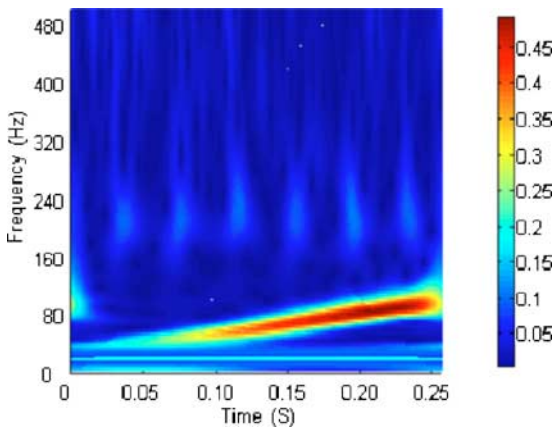
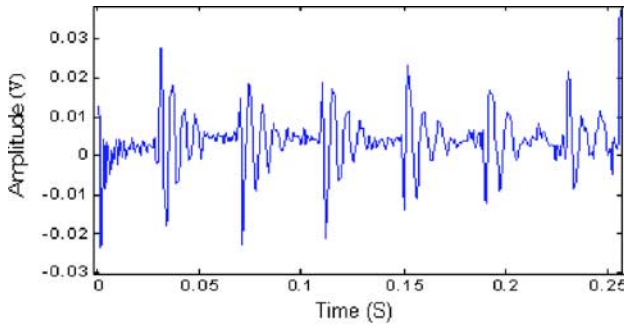
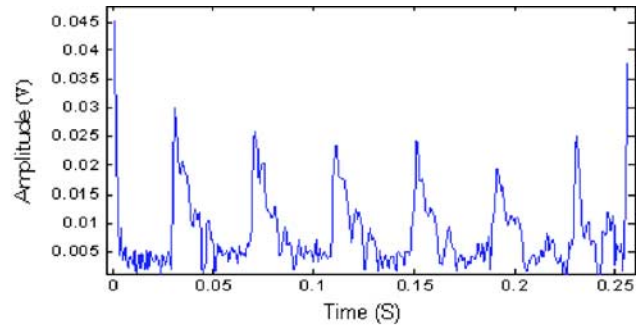


FIG. 5—The S-transform of the simulated signal.

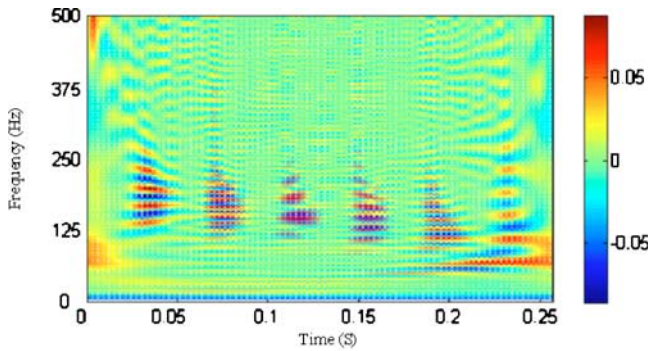
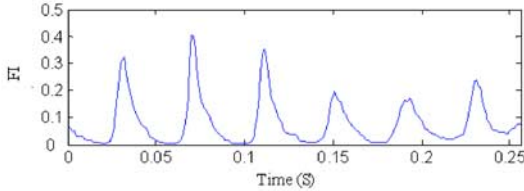


(a) The data on the diagonal of HTT matrix



(b) The envelope of the data in Fig. 6 (a)

FIG. 6—The HTT-transform of the simulated signal [19].

(a) The real parts of S-transform coefficients of modulating signal  $A(t)$ 

(b) FIs obtained based on the coefficients in Fig. 7 (a)

FIG. 7—The analysis result of the simulated signal using the proposed method.

$$I(x) = \begin{cases} 1, & \text{if } x \text{ is true} \\ 0, & \text{if } x \text{ is false} \end{cases} \quad (11)$$

According to Eq 10, it can be seen that FI is equal to zero if all  $|a_{i,j}|$  are smaller than  $|\bar{a}_j| + 3\sigma_0$ . When the gearbox is healthy, most of the  $|a_{i,j}|$  values will be smaller than  $|\bar{a}_j| + 3\sigma_0$  and thus resulting in a small FI value. When a fault is developing in the gearbox, modulation will become more and more serious as the fault grows, a higher percentage of the  $|a_{i,j}|$  values will be bigger than  $|\bar{a}_j| + 3\sigma_0$ , and FI will be bigger as well. Therefore, FI is expected to reflect fault features. In addition, because both  $a_{i,j}$  and  $\bar{a}_j$  are expected to be dependent on load, the FI value is expected to be less dependent on the load. As a result, the FI is expected to be a robust indicator of the development of fault in a gearbox.

The idea of using data points outside of the three standard deviations of the mean value of a data series as a measure of the property of the data series is not new. Miller defined a so-called fault growth parameter (FGP) as the percentage of data points in the residual error signal that exceed the three standard deviations from the baseline residual signal [23]. The baseline residual signal is the

one collected when a healthy gearbox starts its operation. Lin et al. improved this FGP and proposed FGP1 that was more sensitive to gearbox faults [24]. Both FGP and FGP1 are measures of the properties of the residual vibration signals obtained through an ideal filter. In reality, the speed of a gearbox fluctuates with time. As a result, the meshing frequency, sidebands, and their harmonics fluctuate with time as well. Thus, it is difficult to filter out these frequency components in obtaining the residual signal. However, the proposed FI parameter does not rely on the so-called residual signal. Instead, we use the Hilbert transform and S-transform to process the obtained vibration signals directly.

Figure 1 illustrates how the proposed FI parameter will be obtained from the coefficients of the S-transform. Corresponding to each time position, for instance  $t_1$ , the coefficient of the S-transform is available at each frequency point  $(f_1, f_2, \dots, f_L)$ . The standard deviation of the real parts of these coefficients at each time position can be calculated and we obtain  $\sigma_j$  for  $j=1, 2, \dots, N$ . Assuming that the fault feature will not be present at all these  $N$  time positions, the smallest standard deviation among these  $\sigma_j$  values can be used to measure this healthy status. The  $\sigma_0$  value in Eq 10 can be obtained by  $\sigma_0 = \min\{\sigma_j | j=1, 2, \dots, N\}$ .

Using Eq 10, we can calculate an FI value at each time position, namely,  $FI_1, FI_2, \dots, FI_N$ . The feature indicator  $FI_j$  reflects the number of data points locating outside of  $|\bar{a}_j| + 3\sigma_0$ . Because the vibration components caused by faults usually have higher amplitude, the value of  $|\bar{a}_j|$  at the time position where there is a fault feature will usually have a larger value. To highlight the fault features, we will use the value of  $|\bar{a}_j|$  to modify the feature indicator calculated with Eq 10. The modified feature indicator is expressed by

$$FI_j = \frac{w_j}{L} \sum_{i=1}^L I(|a_{i,j}| > (|\bar{a}_j| + 3\sigma_0)) \quad (12)$$

where  $w_j = |\bar{a}_j| / \sum_{j=1}^N |\bar{a}_j|$ . Therefore, FI represents the proportion of outliers, takes value in the range of [0, 1], and is dimensionless. Equation 12 will be used in subsequent sections to calculate the feature indicators.

For fault feature extraction in gearbox condition monitoring, we are usually interested in the times of impulses and the duration between adjacent impulses. This can be achieved through observation of the obtained  $FI_j$  values. The procedure of the proposed method is shown in Fig. 2.

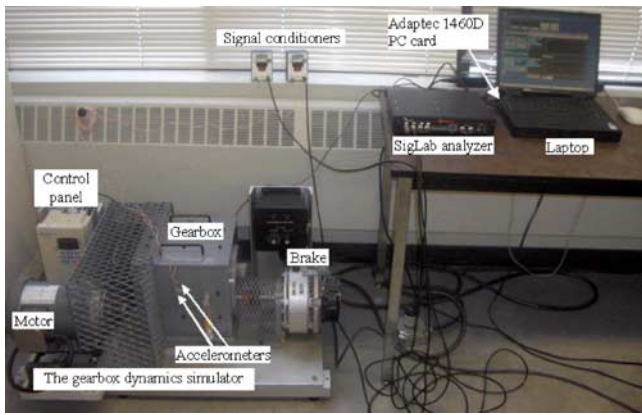


FIG. 8—Diagram of the experiment setup.

TABLE 1—Characteristic frequencies of the gearbox (Hz).

Rotating Frequencies			Meshing Frequencies	
Shaft 1	Shaft 2	Shaft 3	Gears 1 and 2	Gears 3 and 4
14.9	4.96	8.28	238.4	198.67

A tooth is removed by milling.



FIG. 9—The faulty gear missing a single tooth.

## Examples

### Simulated Signals

In order to verify the effectiveness of the proposed method, a simulated signal is analyzed. The simulated signal  $x(t)$  is composed of a series of periodic impulses represented by the function  $0.4e^{-100t} \sin(2\pi 166.7t)$  and its translations in the time domain. The time interval between adjacent impulses is 0.04 s. In addition, the simulated signal also contains a chirp signal represented by

$\sin(300\pi t^2)$ . These two independent sources are shown in Figs. 3(a) and 3(b), respectively. The mixed signals including the impulse component, the chirp component, and a third component represented by  $0.035N(t)$  are shown in Fig. 3(c), where  $N(t)$  is a white Gaussian noise whose power is 1 dB simulated by the `randn` function of Matlab. The length of the simulated signals is 0.256 s.

Because impulses often represent fault features, we are interested in detecting the impulses in the mixed signal. Figure 4 shows the analysis results using the adaptive CWT with four types of mother wavelets [13,25]. Clearly, the results are dependent on the selected mother wavelets. Some impulses are revealed in these figures, while other impulses are still hidden. Figure 5 is the S-transform of the simulated signal directly, where we can see some impulses. Unfortunately, there are also other strong signal components in Fig. 5. This makes it difficult for fault detection by visual inspection. Figure 6 shows the results using HTT method [19]. It is very easy to extract the starting time of each impulse and the time intervals among adjacent impulses in Fig. 6. This shows that HTT is very effective for detection of impulses in the simulated signal. Figure 7 presents the analysis results using the proposed method. Compared with other results in Figs. 4–6, it is easier to find impulses and the time interval of 0.04 s in Fig. 7(b). This shows that the proposed method is more effective than the adaptive CWT and as effective as HTT for identification of impulses in the simulated signal.

### Real Vibration Signals

The experiment setup used in this study is shown in Fig. 8. The gearbox contained four gears, three shafts, and six bearings. Testing was conducted on a two-stage gearbox dynamics simulator driven by a three-horsepower induction motor through a belt. The workload was 3.6 ft-lb. Two accelerometers, PCB 352C67, were mounted on the gearbox in vertical and horizontal directions. The vibration data with a length of 1.6 s was acquired by a DSP Siglab 20-42 signal analyzer and a Dell Inspiron 7500 laptop computer at a sampling frequency of 1280 Hz. Table 1 lists the characteristic frequencies of the gearbox. In order to simulate gear fault, a single tooth of the gear installed on the output shaft was removed by a milling machine, shown in Fig. 9. This gear with catalog number NH24A was produced by Boston Gear Company. The dimensions can be found in Ref. [26]. We changed the gear face width to 0.016 m in order to keep the face the same as its meshing gear in this experiment.

One of the collected raw vibration signals is shown in Fig. 10. Because the faulty gear was on the output shaft, we expect to find

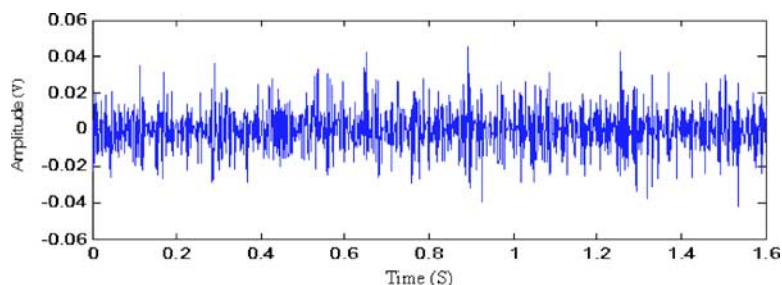


FIG. 10—The raw vibration signal collected from an abnormal gearbox.

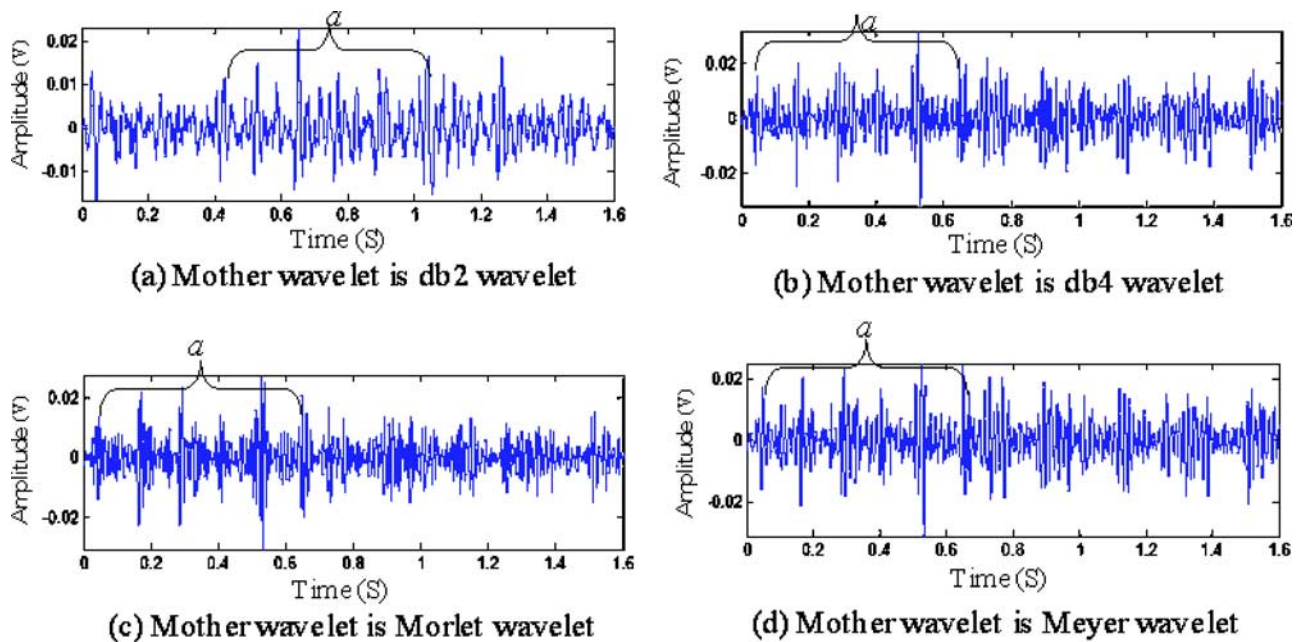


FIG. 11—The analysis results obtained by the adaptive CWT.

impulses with a period of  $1/8.28 \text{ Hz} = 0.1208 \text{ s}$  in the vibration signal. We also anticipate that some slipping of the belt transmission may be occurring as the vibration data were collected. Therefore, the impulses produced by the faulty gear on the output shaft should have a period of approximately  $0.1208 \text{ s}$ .

The analysis results of this vibration signal using the adaptive CWT are shown in Fig. 11. Several impulses of approximately equal time-interval are obvious during the periods marked “a” in Fig. 11. The results obtained by CWT depend heavily on the choice of the mother wavelet. The analyzed results using S-transform and HTT-transform are shown in Figs. 12(a)–12(c), respectively. In Fig. 12(a), it is impossible to identify impulses of relatively equal time intervals. In Figs. 12(b) and 12(c), several impulses of relatively equal time-intervals are present in the periods marked “a” and “b.” Because of the fluctuations of these impulses in Figs. 12(b) and 12(c), the measurement of the time intervals between adjacent impulses requires strong practical experience.

Figure 13(a) shows the analysis results using S-transform of modulating signal  $A(t)$ . In this figure, we cannot identify the equal interval impulses clearly that can reflect the gearbox faults. Especially, it is hard to explain these impulses in the circles shown in Fig. 13(a). Figure 13(b) presents the analysis results, FIs, obtained by the proposed method. In this figure, many individual peaks are present. The time intervals between  $a_i$  and  $a_{i+1}$  ( $i=1, 2, \dots, 13$ ) are very close to  $0.1208 \text{ s}$ . Compared with the plots in Figs. 11, 12, and 13(a), the time intervals between adjacent impulses are easier to identify in Fig. 13(b) by visual inspection. This makes it easier for novice operators to extract fault features with a period of  $0.1208 \text{ s}$  from this plot. We also analyzed the data collected when the input speed and workload were changed to other specific values in order to reflect the variability in practice. Fault features can be extracted effectively by the proposed method as well.

A healthy gear without any faulty tooth was used to replace the faulty gear in the above gearbox. Under the same input speed and

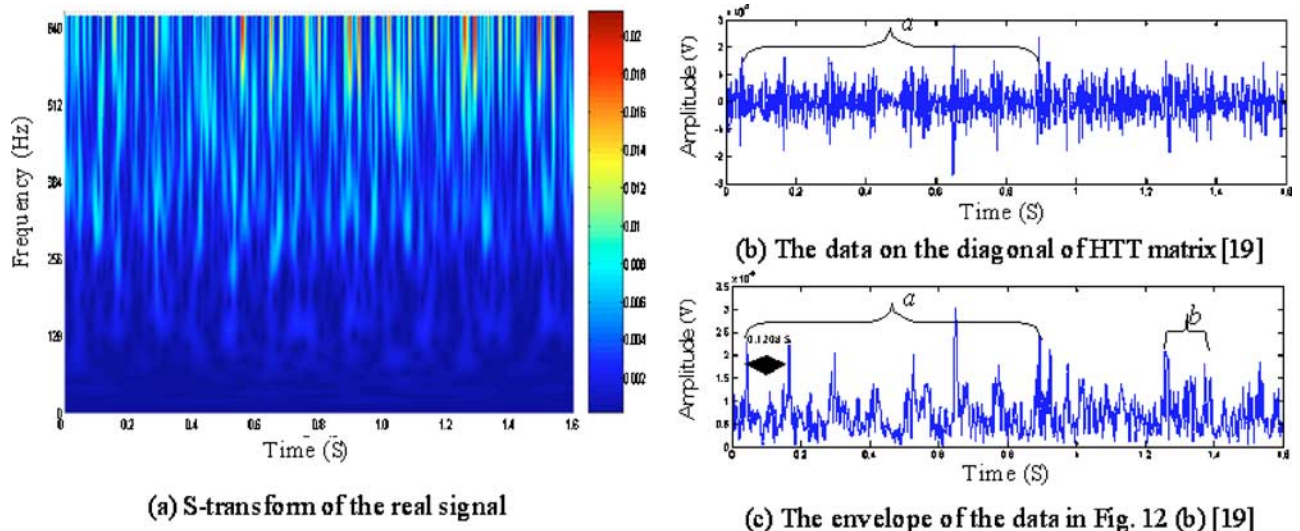


FIG. 12—The analysis results using S-transform and HTT-transform, respectively.

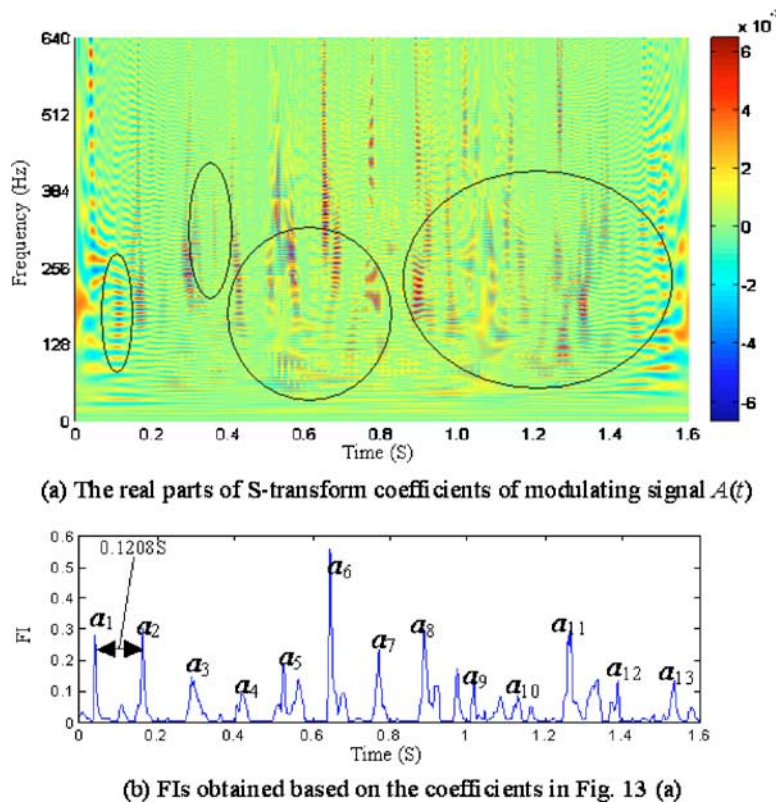


FIG. 13—The analysis result of the abnormal vibration signal using the proposed method.

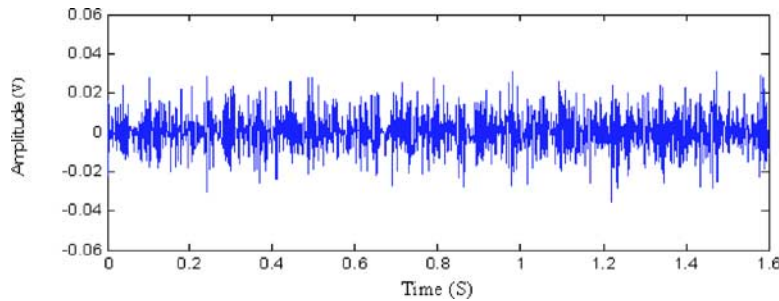


FIG. 14—The raw vibration signal collected from a normal gearbox.

workload, vibration signals were collected. In order to evaluate the proposed method further, we analyzed the obtained normal vibration signals. One of the normal vibration signals is shown in Fig. 14. The analysis result obtained by the proposed method is shown in Fig. 15. Comparing the signals in Figs. 10 and 14, the vibration amplitudes of faulty gearbox are bigger. Comparing the analysis results in Figs. 13(b) and 15(b), we can clearly find that there are no equal-period impulse present in Fig. 15(b). Additionally, all the FIs are bigger than 0.1 in Fig. 13(b), which reflect the fault signatures. However, the maximum amplitude is only 0.084 in Fig. 15(b) and all the FIs are smaller than 0.1. Therefore, according to the value of FI, we can identify the health condition of gearboxes.

## Conclusions

The Hilbert transform, the S-transform, and a feature indicator are combined together to extract fault features. The modulation issue

can be addressed by Hilbert transform while the nonstationarity issue can be addressed by S-transform. The proposed feature indicator is used to measure the properties of the S-transform coefficients in order to disclose fault features directly. The simulated signal and the real vibration signals collected in the lab environment were analyzed. The proposed feature indicator is effective to identify fault and normal conditions of gearboxes. Compared with CWT, S-transform, HTT transform, respectively, the proposed method is more effective to reveal impulse information and does not require the operators to have a lot of diagnostic experience. Therefore, combining signal processing methods and statistical analysis methods has great potential for effective fault detection. In the next step, we plan to refine the proposed method using different gear fault modes with different deterioration levels. Varying speed or workload conditions may be considered as well to reflect more complicated work environments.

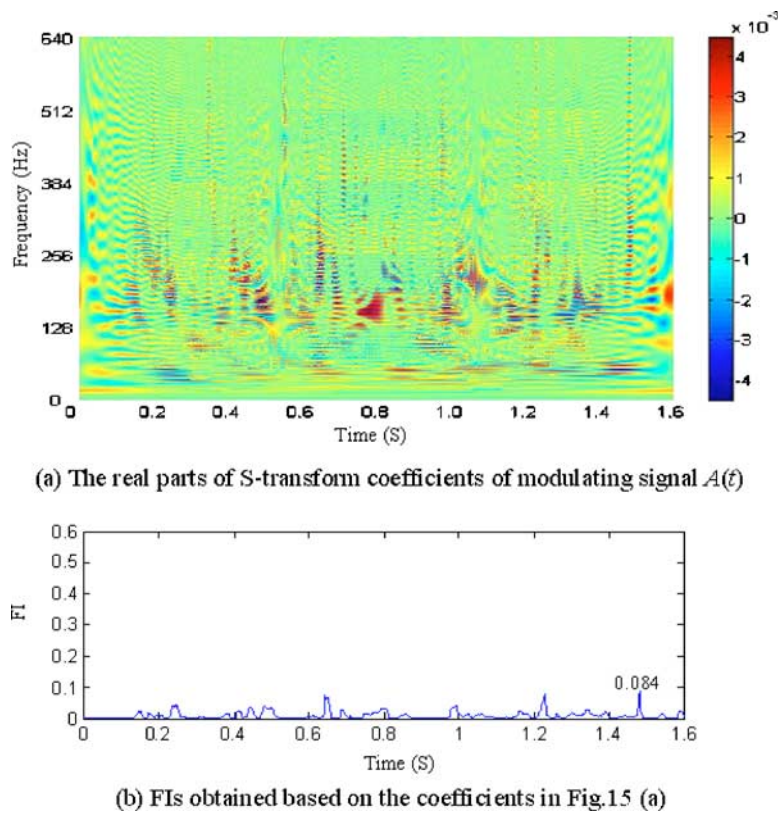


FIG. 15—The analysis result of the normal vibration signal using the proposed method.

### Acknowledgments

The work reported in this paper was supported by the Natural Sciences and Engineering Research Council of Canada (NSERC) and the Open Fund of the State Key Laboratory of Mechanical System and Vibration of Shanghai Jiaotong University under grant VSN-2006-03. We thank the anonymous referees for their many constructive comments.

### References

- [1] Huang, H. Z., "Reliability Evaluation of a Hydraulic Truck Crane Using Field Data with Fuzziness," *Microelectron. Reliab.*, Vol. 36, No. 10, 1996, pp. 1531–1536.
- [2] McFadden, P. D., "Detecting Fatigue Cracks in Gears by Amplitude and Phase Demodulation of the Meshing Vibration," *ASME J. Vib., Acoust., Stress, Reliab. Des.*, Vol. 108, 1986, pp. 165–170.
- [3] Brennan, M. J., Chen, M. H., and Reynolds, A. G., "Use of Vibration Measurements to Detect Local Tooth Defects in Gears," *J. Sound Vib.*, Vol. 31, No. 1, 1997, pp. 12–17.
- [4] Wang, W. Q., Ismail, F., and Golnaraghi, M. F., "Assessment of Gear Damage Monitoring Techniques Using Vibration Measurements," *Mech. Syst. Signal Process.*, Vol. 15, No. 5, 2001, pp. 905–922.
- [5] Pan, M. C., Sas, P., and Brussel, H. V., "Nonstationary Time-Frequency Analysis for Machine Condition Monitoring," *Proceedings of 3rd IEEE Signal Processing Society International Symposium on Time-Frequency and Time-Scale Analysis*, 1996, pp. 477–480.
- [6] Hambaba, A., Huff, E., and Kaul, U., "Time-scale Local Approach for Vibration Monitoring," *Aerospace Conference, 2001, IEEE Proceedings*, Vol. 7, 2001, pp. 7-3201–7-3209.
- [7] Lee, S. K., "Higher Order Time-Frequency Analysis as a Tool for Health Monitoring," *Key Eng. Mater.*, Vol. 245–249, 2003, pp. 175–182.
- [8] Peng, Z. K., and Chu, F. L., "Application of the Wavelet Transform in Machine Condition Monitoring and Fault Diagnostics: A Review with Bibliography," *Mech. Syst. Signal Process.*, Vol. 18, No. 2, 2004, pp. 199–221.
- [9] Kaewkongka, T., Au, Y. H. J., Rakowski, R. T., and Jones, B. E., "A Comparative Study of Short Time Fourier Transform and Continuous Wavelet Transform for Bearing Condition Monitoring," *International Journal of COMADEM*, Vol. 6, No. 1, 2003, pp. 41–48.
- [10] McFadden, P. D., and Wang, W. J., "Analysis of Gear Vibration Signatures by the Weighted Wigner-ville Distribution," *International Conference on Vibrations in Rotating Machinery, Institution of Mechanical Engineers, Bath*, 1992, pp. 387–393.
- [11] Choi, H. and Williams, W., "Improved Time-frequency Representation of Multicomponent Signals Using Exponential Kernels," *IEEE Trans. Acoust., Speech, Signal Process.*, Vol. 37, 1989, pp. 862–871.
- [12] Staszewski, W. J. and Tomlinson, G. R., "Application of the Wavelet Transform to Fault Detection in a Spur Gear," *Mech. Syst. Signal Process.*, Vol. 8, No. 3, 1994, pp. 289–307.
- [13] Lin, J. and Zuo, M. J., "Gearbox Fault Diagnosis Using Adaptive Wavelet Filter," *Mech. Syst. Signal Process.*, Vol. 17, No. 6, 2003, pp. 1259–1269.
- [14] Fan, X. and Zuo, M. J., "Gearbox Fault Detection Using Em-

- pirical Mode Decomposition,” *Proceedings of the ASME Non-destructive Evaluation Engineering Division*, Vol. 25, 2004, pp. 37–45.
- [15] Fan, X. and Zuo, M. J., “Gearbox Fault Detection Using Hilbert and Wavelet Packet Transform,” *Mech. Syst. Signal Process.*, Vol. 20, No. 4, 2006, pp. 966–982.
- [16] Huang, N. E., Shen, Z., Long, S. R. et al., “The Empirical Mode Decomposition and the Hilbert Spectrum for Nonlinear and Non-stationary Time Series Analysis,” *Proceedings of the Royal Society of London*, Vol. 454A, 1998, pp. 903–995.
- [17] Stockwell, R. G., Mansinha, L., and Lowe, R. P., “Localization of the Complex Spectrum: The S-Transform,” *IEEE Trans. Acoust., Speech, Signal Process.*, Vol. 44, No. 4, 1996, pp. 998–1001.
- [18] Dash, P. K., Panigrahi, B. K., and Panda, G., “Power Quality Analysis Using S-transform,” *IEEE Transactions on Power Delivery*, Vol. 18, No. 2, 2003, pp. 406–411.
- [19] Fan, X. and Zuo, M. J., “Gearbox Fault Detection Using Hilbert and TT-transform,” *Key Eng. Mater.*, Vol. 293–294, 2005, pp. 78–86.
- [20] Hahn, S. L., *Hilbert Transform in Signal Processing*, Artech House, London, 1996.
- [21] Zheng, H., Li, Z., and Chen, X., “Gear Fault Diagnosis Based on Continuous Wavelet Transform,” *Mech. Syst. Signal Process.*, Vol. 16, No. 2–3, 2002, pp. 447–457.
- [22] Ferris-Prabhu, A. V., “New Approach to Improving Product Quality,” *Mach. Des.*, Vol. 62, No. 23, 1990, pp. 98–99.
- [23] Miller, A. J., “A New Wavelet Basis for the Decomposition of Gear Motion Error Signals and Its Application to Gearbox Diagnostics,” Thesis, The Pennsylvania State University.
- [24] Lin, D., Wiseman, M., Banjevic, D., and Jardine, A. K. S., “An Approach to Signal Processing and Condition-based Maintenance for Gearboxes Subject to Tooth Failure,” *Mech. Syst. Signal Process.*, Vol. 18, No. 5, 2004, pp. 993–1007.
- [25] Misiti, M., Misiti, Y. et al., *Wavelet Toolbox User's Guide*, MathWorks, Inc..
- [26] [http://www.bostongear.com/pdf/upload/lit/P-1482-BG\\_pg006-015\\_025-034.pdf](http://www.bostongear.com/pdf/upload/lit/P-1482-BG_pg006-015_025-034.pdf)